J Biomol NMR (2009) 44:101–105
DOI 10.1007/s10858-009-9323-1

COMMUNICATION

HNHC: a triple resonance experiment for correlating the H2, N1(N3) and C2 resonances in adenine nucleobases of ^{13}C-, ^{15}N-labeled RNA oligonucleotides

Jörg Rinnenthal · Harald Schwalbe

Received: 23 March 2009 / Accepted: 24 April 2009 / Published online: 8 May 2009

Abstract A novel NMR pulse sequence has been developed that correlates the H2 resonances with the C2 and the N1 (N3) resonances in adenine nucleobases of ^{13}C, ^{15}N labeled oligonucleotides. The pulse scheme of the new 3D-HNHC experiment is composed of a ^{2}J-^{15}N-HSQC and a ^{1}J-^{13}C-HSQC and utilizes large ^{2}J(H2, N1(N3)) and ^{1}J(H2, C2) couplings. The experiment was applied to a medium-size ^{13}C, ^{15}N-labeled 36mer RNA. It is useful to resolve assignment ambiguities occurring especially in larger RNA molecules due to resonance overlap in the ^{1}H-dimension. Therefore, the missing link in correlating the imino H3 resonances of the uracils across the AU base pair to the H8 resonances of the adenines via the novel pulse sequence and the TROSY relayed HCCH-COSY (Simon et al. in J Biomol NMR 20:173–176 2001) is provided.

Keywords NMR spectroscopy · Isotope labeled RNA · Pulse sequence · NMR resonance assignment

The availability of isotope labeled RNA oligonucleotides (Batey et al. 1992; Nikonowicz et al. 1992; Quant et al. 1994; Batey et al. 1995) turned NMR spectroscopy into a powerful tool to determine structure and dynamics of RNAs up to a size of 100 nucleotides (Varani and Tinoco 1991; Varani et al. 1996; Wijmenga 1998; Cromsigt et al. 2001; Fürtig et al. 2003). Heteronuclear NMR experiments allow resonance assignment of the NMR active ^{1}H, ^{13}C, ^{15}N and ^{31}P nuclei which is a prerequisite for further structural and dynamical studies on RNA molecules. In general, most of the experiments use large heteronuclear couplings in order to create a through-bond correlation of distinct nuclei. However, in some cases these couplings are too small and transverse relaxation especially in the nucleobases is too fast so that NOE-based strategies complement the set of suitable resonance assignment experiments. Usually resonance assignment starts with an NOE-based correlation of the imino resonances, since imino resonances show high dispersion especially in the ^{1}H dimension. The number of peaks is comparably small because only those imino groups give rise to an NMR signal that participate in a hydrogen bridge. From the imino signal, the assignment is extended to the non-exchangeable aromatic protons and then to the H1′ resonances of the ribose moiety (Varani et al. 1996; Wijmenga 1998; Fürtig et al. 2003).

The assignment of the adenine and cytosine bases, which do not possess imino groups, is more difficult. It relies on correlations across the base pair, starting from the imino resonances of guanine and uracil nucleobases. For the adenine nucleobases, the assignment of H2 protons in ^{13}C, ^{15}N-labeled RNA is usually obtained from the strong NOE between the uracil H3 and the adenine H2 in an AU base pair and assignment of the adenine N1 is usually obtained via the HNN-COSY experiment in which the uracil H3-N3 signal is correlated to the N1 resonance of the adenine (Dingley and Grzesiek 1998). Then, it is possible to assign the H2-N1 resonance pair in the adenine nucleobase in the ^{2}J-^{15}N-HSQC unambiguously. The adenine through-base connectivity is most suitably obtained

Electronic supplementary material The online version of this article (doi:10.1007/s10858-009-9323-1) contains supplementary material, which is available to authorized users.

J. Rinnenthal · H. Schwalbe (✉)
Institute for Organic Chemistry and Chemical Biology,
Center for Biomolecular Magnetic Resonance,
Johann Wolfgang Goethe-University, Max-von-Laue-Strasse 7,
60438 Frankfurt/Main, Germany
e-mail: schwalbe@nmr.uni-frankfurt.de

via the TROSY relayed HCCH-COSY experiment (Simon et al. 2001) which allows the assignment of the H2-C2 and the H8-C8 signals to the same nucleobase via the correlation to the C4, C5 and C6 resonances. Base connectivity can also be obtained using a 2D ^{1}H, ^{13}C-HMBC experiment (van Dongen et al. 1996) which is recommended for smaller RNA or DNA molecules where spectral overlap in the proton dimension only rarely occurs.

However, there is the need to correlate the H2-N1 resonances of the ^{2}J-^{15}N-HSQC to the C2 resonances. Such correlation can be accomplished with the ^{13}C-HSQC as long as there is no signal overlap in the ^{1}H dimension. However, to resolve signal overlap, it is necessary to correlate signals observed in the ^{2}J-^{15}N-HSQC to the C2 resonances. Such correlation cannot be achieved in an HCN experiment (Sklenar et al. 1993), since the ^{1}J(C2, N1(3))-coupling is smaller than 1 Hz (Fig. 1) (Fiala et al. 2004). Therefore, we developed a novel pulse sequence that correlates the three nuclei H2, C2 and N1(N3) in the adenine nucleobase by utilizing the strong ^{2}J(H2, N1(3)) and ^{1}J(H2, C2) couplings (as depicted in Fig. 1) (Fiala et al. 2004).

The 3D-(^{15}N, ^{13}C, ^{1}H)-HNHC experiment (Fig. 2) is a combination of a ^{13}C-HSQC and a ^{2}J-^{15}N-HSQC. It is designed to transfer the magnetization in a double out and back manner from the H2 to the N1(3) and the C2 using single quantum coherences (Fig. 1). Besides the H2–C2–N1(3) correlation, the experiment also provides the H8–C8–N7 correlation in guanine and adenine bases (Fig. 1) and an adjustment of the ^{15}N carrier frequency from 221 to 170 ppm gives also the correlation of the H8–C8–N9 resonances. However, the common HCN experiment (Sklenar et al. 1993) is able to produce the H8–C8–N9 correlation as well. So we decided only to use hard pulses on the ^{15}N channel (Fig. 2), since these pulses are not short enough to excite the N9 resonances as long as the ^{15}N carrier frequency is set to 221 ppm. Therefore, the ^{15}N-spectral-width in the ω_1-dimension can be reduced to 24 ppm and the experiment can be run with a higher resolution without further hassle.

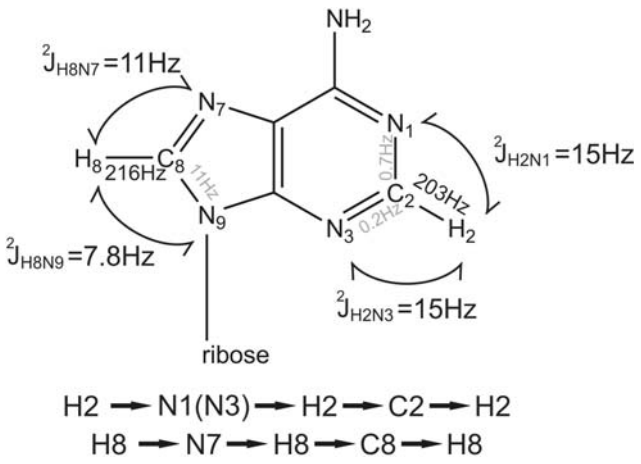

Fig. 1 Schematic representation of the scalar couplings involved in the coherence transfer pathway of the 3D-HNHC experiment in adenine (Fiala et al. 2004). The ^{1}J(C, N) couplings that are used for the HCN experiment are shown in *gray* (Fiala et al. 2004). The schematic coherence transfer pathways of the 3D-HNHC pulse sequence are also indicated

In the 3D-(^{15}N, ^{13}C, ^{1}H)-HNHC pulse sequence (Fig. 2), the coherence $2H2_zN1(3)_z$ at time point **a** is created via an INEPT step utilizing the strong ^{2}J(H2, N1(N3)) coupling (15 Hz). Between **a** and **b** the coherence is labeled with the ^{15}N chemical shift. In the refocusing INEPT, evolution of the ^{2}J(H2, N1(N3)) coupling is concatenated with the evolution of the ^{1}J(H2, C2) coupling (200 Hz), leading to the coherence $2H2_zC2_z\exp(i\omega_{N1(3)}t_1)$ at time point **c**. C2 chemical shift evolution occurs between **c** and **d**. Finally the ^{1}J(H2, C2) coupling (200 Hz) is refocused resulting in $H2_x\exp(i\omega_{N1(3)}t_1)\exp(i\omega_{C2}t_2)$ inphase magnetization in **e**. Neglecting relaxation effects, optimal sensitivity is achieved by setting the delay τ to 16 ms ($1/(4*^{2}J_{H2N1(3)})$). However, for larger RNA molecules showing high R_2 rates of the H2 protons, the delay τ has to be optimized towards shorter delays in order to obtain optimal sensitivity. The pulse sequence illustrated in Fig. 2 contains a soft Watergate water suppression element (Piotto et al. 1992), which makes the pulse sequence applicable to H_2O-samples. Although the pulse sequence can be applied to a D_2O sample, we optimized gradients and water flip back pulses on an H_2O sample so that the important experiments such as 2D NOESY, HNN-COSY, HNHC and TROSY relayed HCCH-COSY can be performed on the same sample. Additionally to this implementation, an echo/antiecho sensitivity enhanced (Fig. S1) (Kay et al. 1992) and an echo/antiecho TROSY (Fig. S2) version (Nietlispach 2005) of the 3D-(^{15}N, ^{13}C, ^{1}H)-HNHC experiment have been developed. The pulse sequences are part of the supplementary material. We found that the soft Watergate version has a slightly higher sensitivity than the echo/antiecho sensitivity enhanced version. For the 36mer test RNA, the TROSY implementation is less sensitive by a factor of 2, but the signals have smaller line widths especially in the ^{13}C dimension. All the soft pulses, applied on the water frequency (small gray semi-ellipses, Fig. 2), are optimized to reduce the intensity of the water signal. They are applied in a way that the water magnetization is stored along z. Gradients are applied to eliminate artifacts and suppress radiation damping of the water signal during the time periods in which the water magnetization is transverse or along $-z$. During the chemical shift evolution periods the water magnetization is along $-z$ for time periods of $t_1/2$ and $t_2/2$, respectively. Therefore, bipolar gradients (Sklenar 1995) are used to suppress radiation damping during t_1 and t_2.

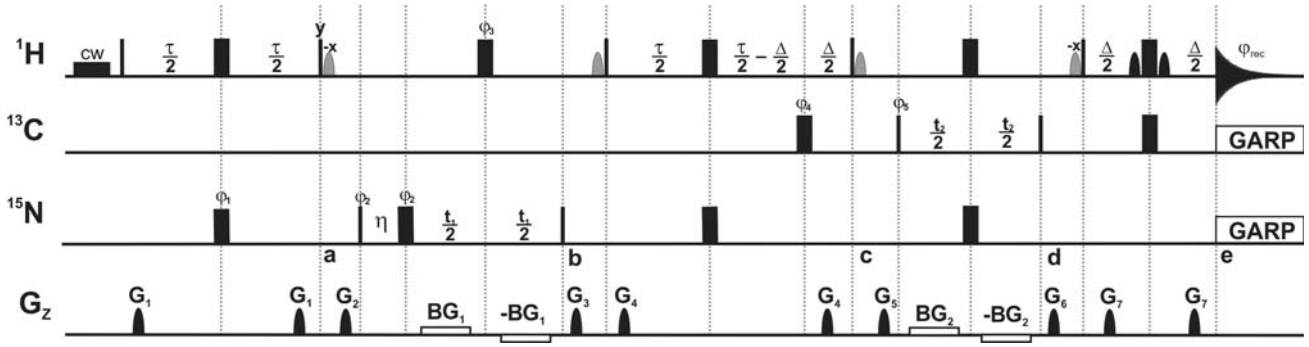

Fig. 2 Pulse sequence of the 3D-HNHC experiment in the soft Watergate water suppression (Piotto et al. 1992) implementation. *Narrow* and *wide filled bars* correspond to rectangular 90° and 180° pulses applied with RF field strengths of 25.5 kHz (^{1}H), 19.5 kHz (^{13}C), 6.95 kHz (^{15}N), respectively. Gradients (G_{1-7}) are indicated as *black filled semi-ellipses*. Bipolar gradients (BG_1, BG_2) (Sklenar 1995) are indicated as *unfilled black rectangles*. The default pulse phase is *x*. The pulse sequence was optimized on a Bruker spectrometer with the Bruker typical phase settings (Roehrl et al. 2005). The *wide filled bar* indicated with cw is an optional presaturation pulse on the water resonance. Fixed delays are adjusted as follows: $\Delta = 1.25\,\text{ms}(1/(2*^{1}J_{H2C2}))$, $\tau = 16\,\text{ms}(1/(4*^{2}J_{H2N1(3)}))$, $\eta = 20.4$ µs (length of the 180° pulse on the ^{1}H channel) + $t_1(0) = 26.4$ µs. The proton carrier frequency is centered at the water frequency (4.7 ppm). The carbon carrier frequency is set to 144 ppm (middle between C2 and C8) and the nitrogen carrier frequency is set to 221 ppm (middle between N1, N3 and N7). At 700 MHz, band selective pulses are set as follows: 90° square pulse (*small gray semi-ellipse*, water flipback) 1.5 ms, 90° square pulse (*small black semi-ellipse*, soft Watergate water suppression) 0.85 ms. Asynchronous GARP decoupling (Shaka et al. 1985) on the carbon and the nitrogen channel is used to suppress heteronuclear scalar couplings during acquisition. The pulse field gradients G_1–G_7 have *sine bell shaped* amplitudes. G_1–G_6 are 1 ms and G_7 is 200 µs in length. All gradients are applied along the *z*-axis and have the following strengths: G_1: 41%, G_2: 7%, G_3: 11%, G_4: 53%, G_5: 23%, G_6: 29%, G_7: 85, 100% of gradient strength corresponds to 55 Gauss/cm. The bipolar pulse field gradients BG_1 and BG_2 (Sklenar 1995) are applied along the *z*-axis, have *rectangular shaped* amplitude and are $t_1/2$ (BG_1) and $t_2/2$ (BG_2) in length. The bipolar gradients have the following strengths: BG_1: 2%, BG_2: 3%. Phase cycling: $\varphi_1 = x$; $\varphi_2 = x, -x$; $\varphi_3 = 2(x), 2(-x)$; $\varphi_4 = x$; $\varphi_5 = 4(x), 4(-x)$; $\varphi_6 = x$; $\varphi_{rec} = x, -x, x, -x, -x, x, -x, x$. φ_1 and φ_2 are incremented in a States-TPPI (Marion et al. 1989) manner to achieve quadrature detection in the ^{15}N (ω_1) dimension and φ_4 and φ_5 are incremented according to States-TPPI (Marion et al. 1989) to achieve quadrature detection in the ^{13}C (ω_2) dimension

We also investigated the alternative option to obtain the required correlations by exciting double- and zero-quantum (DQ/ZQ) coherence such as $4H2_zN1(3)^{+/-}C2^{+/-}$ and $4H2_zN1(3)^{+/-}C2^{-/+}$ and evolve sums and differences of the chemical shifts of the N1(3) and C2 nuclei in a concatenated manner. Such an experiment would be shorter for one CH-INEPT transfer period than the SQ version we propose. However, the DQ/ZQ experiment requires post-acquisition processing and a more elaborate phase cycle to separate DQ and ZQ coherences.

The new pulse sequence was applied to a 0.7 mM ^{13}C, ^{15}N adenosine-, cytidine-labeled 36mer RNA oligonucleotide (Fig. 3b) sample in D_2O. Water suppression was optimized on a different sample. Slices taken from the spectrum of the 3D-(^{15}N, ^{13}C, ^{1}H)-HNHC experiment are shown in Fig. 3a. Each slice shows two peaks, representing the H2-C2-N1 and H2-C2-N3 correlations. Figure 3c shows a ^{2}J-^{15}N-HSQC recorded under the same conditions as the 3D-(^{15}N, ^{13}C, ^{1}H)-HNHC experiment. A comparison of Fig. 3a and Fig. 3c indicates that all the signals present in the ^{2}J-^{15}N-HSQC are also present in the 3D-(^{15}N, ^{13}C, ^{1}H)-HNHC experiment. Consequently, our data show that the experiment is applicable to mid-size RNA oligonucleotides. However, given the high S/N-ratio of the experiment it should be readily applicable also to larger RNAs. Furthermore, Fig. 3 shows that signals overlapping in the proton dimension, especially A22/A16 and A29/A7, can be resolved in the 3D-(^{15}N, ^{13}C, ^{1}H)-HNHC experiment and the assignment ambiguities can be removed successfully.

In conclusion, we have introduced a novel method to correlate the H2-C2-N1 and H2-C2-N3 resonances of the adenine nucleobases in ^{13}C, ^{15}N labeled oligonucleotides. The new method simplifies the assignment of the adenine nucleobases since it reduces assignment ambiguities occurring especially in larger RNA molecules due to signal overlap. By correlating the H2-N1 resonances with the C2 resonances, the new method provides the missing link for correlating the imino H3 resonances of the uracil nucleobases across the AU base pairs to the H2 resonances and subsequently to the H8 resonances of the adenine nucleobases.

Supplementary material

The pulse schemes for an echo/antiecho sensitivity enhanced version and an echo/antiecho TROSY version of the 3D-(^{15}N, ^{13}C, ^{1}H)-HNHC experiment are part of the supplementary material.

Acknowledgments The work has been supported by the state of Hesse (Center for Biomolecular Magnetic Resonance, BMRZ) and the DFG (Sonderforschungsbereich 579: RNA–ligand-interactions).

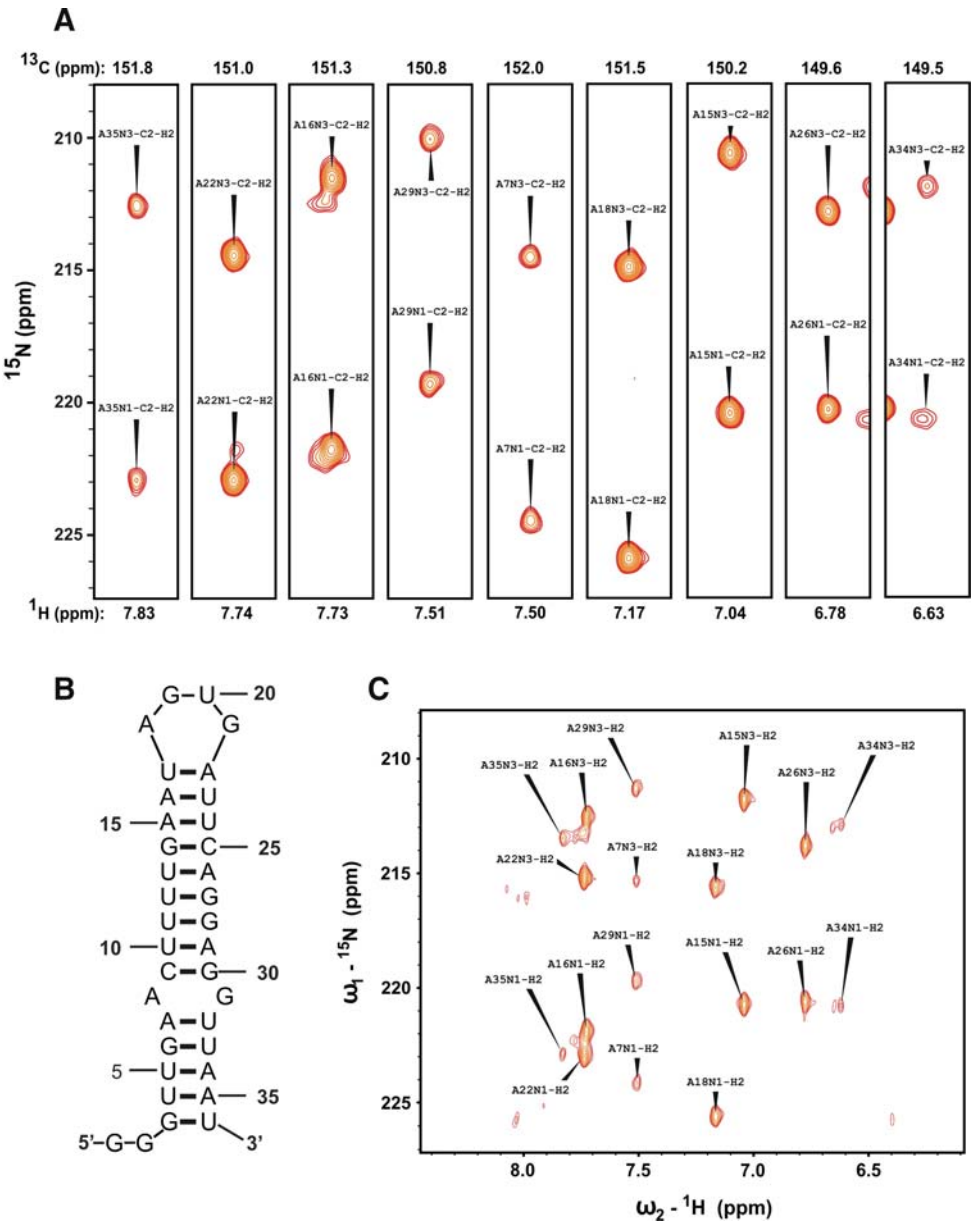

Fig. 3 **a** Spectrum of the 3D-HNHC experiment in the *strip* plot representation with the ^{13}C (ω_2) dimension orthogonal to the paper plane. The spectrum was recorded at $T = 20$°C for 41 h on a Bruker 700 MHz spectrometer equipped with a 5 mM TXI cryogenic probe. Spectra were recorded with 88 (^{15}N) * 148 (^{13}C) increments, each with 8 scans. Spectral widths in the three dimensions were set to 24 ppm (^{15}N), 18 ppm (^{13}C) and 16 ppm (^{1}H). A selectively adenosine, cytidine ^{13}C, ^{15}N-labeled sample with a concentration of 0.7 mM in a D_2O buffer was used. **b** Secondary structure of the 36mer RNA hairpin 2 derived from the transcribed 5′-UTR (untranslated region) of the *Salmonella* agsA gene (Waldminghaus et al. 2007). **c** Section of a 2D-^{2}J-^{15}N-HSQC spectrum from the RNA molecule depicted in (**b**) recorded for 1.8 h under the same conditions than the 3D-HNHC experiment. 512 increments were recorded with 8 scans each. Spectral widths were set to 140 ppm (^{15}N) and 16 ppm (^{1}H). The ^{15}N and ^{13}C carrier frequencies were set to 210 ppm (^{15}N), 144 ppm (^{13}C) and 4.7 ppm (^{1}H). GARP decoupling (Shaka et al. 1985) was applied to the carbon channel during acquisition

We thank Dr. Birgit Klinkert and Professor Dr. Franz Narberhaus (Institute for Biology of Microorganisms, Ruhr-University, Bochum) for providing us with an initial pUC19 plasmid containing the 4U-hp2-wt 36mer RNA template.

References

Batey RT, Inada M, Kujawinski E, Puglisi JD, Williamson JR (1992) Preparation of isotopically labeled ribonucleotides for multidimensional NMR spectroscopy of RNA. Nucleic Acids Res 20:4515–4523

Batey RT, Battiste JL, Williamson JR (1995) Preparation of isotopically enriched RNAs for heteronuclear NMR. Methods Enzymol 261:300–322

Cromsigt J, van Buuren B, Schleucher J, Wijmenga S (2001) Resonance assignment and structure determination for RNA. Methods Enzymol 338:371–399

Dingley AJ, Grzesiek S (1998) Direct observation of hydrogen bonds in nucleic acid base pairs by internucleotide 2JNN couplings. J Am Chem Soc 120:8293–8297

Fiala R, Munzarova ML, Sklenar V (2004) Experiments for correlating quaternary carbons in RNA bases. J Biomol NMR 29:477–490

Fürtig B, Richter C, Wöhnert J, Schwalbe H (2003) NMR-spectroscopy of RNA. ChemBioChem 4:936–962

Kay L, Keifer P, Saarinen T (1992) Pure absorption gradient enhanced heteronuclear single quantum correlation spectroscopy with improved sensitivity. J Am Chem Soc 114:10663–10665

Marion D, Ikura M, Tschudin R, Bax AJ (1989) Rapid recording of 2D NMR spectra without phase cycling. Application to the study of hydrogen exchange in proteins. J Magn Reson 85:393–399

Nietlispach D (2005) Suppression of anti-TROSY lines in a sensitivity enhanced gradient selection TROSY scheme. J Biomol NMR 31:161–166

Nikonowicz EP, Sirr A, Legault P, Jucker FM, Baer LM, Pardi A (1992) Preparation of ^{13}C and ^{15}N labelled RNAs for heteronuclear multi-dimensional NMR studies. Nucleic Acids Res 20:4507–4513

Piotto M, Saudek V, Sklenar V (1992) Gradient-tailored excitation for single-quantum NMR spectroscopy of aqueous solutions. J Biomol NMR 2:661–665

Quant S, Wechselberger R, Wolter M, Wörner K-H, Schell P, Engels J, Griesinger C, Schwalbe H (1994) Chemical synthesis of ^{13}C-labelled monomers for solid-phase and template controlled enzymatic synthesis of DNA and RNA oligomers. Tetrahedron Lett 35:6649–6652

Roehrl MH, Heffron GJ, Wagner G (2005) Correspondence between spin-dynamic phases and pulse program phases of NMR spectrometers. J Magn Reson 174:325–330

Shaka AJ, Barker PB, Freeman RJ (1985) Computer-optimized decoupling scheme for wideband applications and low-level operation. J Magn Reson 64:547–552

Simon B, Zanier K, Sattler M (2001) A TROSY relayed HCCH-COSY experiment for correlating adenine H2/H8 resonances in uniformly ^{13}C-labeled RNA molecules. J Biomol NMR 20:173–176

Sklenar V (1995) Suppression of radiation damping in multidimensional NMR experiments using magnetic field gradients. J Magn Reson A 114:132–135

Sklenar V, Peterson RD, Rejante MR, Feigon J (1993) Two- and three-dimensional HCN experiments for correlating base and sugar resonances in ^{15}N, ^{13}C-labeled RNA oligonucleotides. J Biomol NMR 3:721–727

van Dongen MJ, Wijmenga SS, Eritja R, Azorin F, Hilbers CW (1996) Through-bond correlation of adenine H2 and H8 protons in unlabeled DNA fragments by HMBC spectroscopy. J Biomol NMR 8:207–212

Varani G, Tinoco I Jr (1991) RNA structure and NMR spectroscopy. Q Rev Biophys 24:479–532

Varani G, Aboul-ela F, Allain FH-T (1996) NMR investigation of RNA structure. Prog Nucl Magn Reson Spectrosc 29:51–127

Waldminghaus T, Heidrich N, Brantl S, Narberhaus F (2007) FourU: a novel type of RNA thermometer in *Salmonella*. Mol Microbiol 65:413–424

Wijmenga SS, van Buuren BNM (1998) The use of NMR methods for conformational studies of nucleic acids. Prog Nucl Magn Reson Spectrosc 32:287–387